Rover Publications
United International Journal of Engineering and Sciences (UIJES)
An International Peer-Reviewed (Refereed) Engineering and Science Journal
Impact Factor: 7.984 (SJIF) Vol-4, Issue- 2, 2024 ISSN: 2582-5887, www.uijes.com

The Role of Thermal Aging in Crack Growth of Lead-Free Solder Interconnects

Samuel Ambosta, USA.
Anuraag Karnik, USA.
Pavan Rajmane, USA.
Dereje Agonafer, USA.

Abstract: Reliability assessment is crucial for determining the longevity of electronic devices, benefiting both manufacturers and consumers by optimizing performance and durability. Lead-free solder joints in electronic components undergo significant changes in microstructure, mechanical properties, and failure behavior when subjected to isothermal aging and thermal cycling. These solder interconnects are particularly vulnerable to fatigue stresses due to reflow processes and harsh environmental conditions, which can accelerate crack propagation. Although some lead-free materials may harden over time, potentially enhancing crack resistance through increased surface roughness, elevated thermal aging generally diminishes the reliability of packages, especially in Pb-free BGA assemblies. Previous studies have indicated that mechanical property alterations in Pb-free solders, influenced by mismatched thermal expansion coefficients (CTEs) among different materials, can lead to failure.

This research investigates the interplay between Stress Intensity Factor (SIF) and crack growth in solder interconnects under varied thermal aging and cycling conditions. Comprehensive experimental tests were conducted across a range of temperatures and durations to assess the thermomechanical properties of solder joints and printed circuitboards (PCBs). Techniques such as Dynamic Mechanical Analysis (DMA) and Thermomechanical Analysis (TMA) were employed. A finite element model was developed to correlate experimental findings with age-related fracture behavior in solder joints. By focusing on a 25 µm circumferential area, the finite element analysis (FEA) computed stress components and their temporal variation across solder ball interconnects. This study not only reduces experimental costs and time but also enhances our understanding of crack propagation by linking crack dimensions, stress evolution, and loading conditions. Insights into thermal loads, stress intensity factors, and crack growth mechanisms are also provided, contributing to improved reliabilityin electronic packaging.

Keywords - Thermal aging, Crack growth, Lead-free solder, Interconnect reliability, Microstructure, Mechanical properties, Fatigue resistance, Thermal cycling

I. INTRODUCTION

1.1 Electronic Packaging

Electronic packaging is a multidisciplinary domain that blends principles from industrial, mechanical, electrical, and materials science. As outlined by Cluff et al. in the Mechanical Engineering Handbook, electronic packaging encompasses the art and science of integrating electronic components to reliably perform designated functions under specific operational conditions. Effective packaging not only provides mechanical support but also ensures efficient heat dissipation, power distribution, and signal integrity, all while protecting against external environmental, chemical, and electromagnetic influences.

1.2 Ball Grid Array (BGA) Package

In Ball Grid Array (BGA) packages, solder balls are arranged in a grid pattern to connect integrated circuits (ICs) to the PCB, leveraging the entire bottom surface of the IC for enhanced electrical and thermal performance. Various BGA types include:

- HSBGA: BGA with a heat spreaderFCBGA: Flip Chip BGA
- CSBGA: Cost-Saving BGAFBGA: Fine Pitch BGA
- μBGA: Micro-BGA, among others.

The benefits of BGA packages include reduced inductance, increased pin counts, improved current distribution, better thermal performance, and auto-registration capabilities. However, these advantages come with challenges, such as soldering difficulties, the complexity of detecting soldering defects, high equipment costs, and concerns about hand soldering reliability.

Figure 3. Ball Grid Array Package

1.3 Reliability Issues with Solder Interconnects

Recent advancements in technology have led to the production of smaller, high-density packages featuring tiny solder balls with reduced spacing. These miniature solder interconnects are particularly sensitive to variations in solder alloy composition and the formation of intermetallic compounds (IMC). Lead-free solder joints, such as those using Sn-Ag-Cu (SAC) alloys, experience significant alterations in microstructure, mechanical properties, and failure modes due to thermal aging and temperature cycling. This aging process can adversely affect the cycle life of solder joints and increase their susceptibility to fracture.

1.4 Motivation

Understanding crack formation under thermo-mechanical loading is vital, given the challenges posed by IMC growth and variations in solder alloy composition. This study focuses on the fracture behavior of SAC solders, which are widely used in contemporary electronic packages, to assess their reliability.

1.5 Objective and Scope

This research employs a combination of experimental methods and finite element analysis (FEA) to investigate critical crack growth in solder interconnects subjected to thermal aging and cycling. Utilizing a multi-level finite element (MLFE) approach in ANSYS WORKBENCH 18.0, the study explores fracture propagation under thermal cycling conditions as per JESD22-A104D standards. The analysis includes computations of the J-integral and Stress Intensity Factor (SIF) to identify significant cracks and their modes of fracture. Additionally, the study evaluates the effects of thermal loads and crack behavior on plastic work and cycles leading to package failure.

II. LITERATURE REVIEW

The reliability of lead-free solder interconnects in electronic packaging has become a crucial area of research, particularly in the context of thermal aging and its influence on crack growth behavior. With

Impact Factor: 7.984 (SJIF) Vol-4, Issue- 2, 2024 ISSN: 2582-5887, www.uijes.com

the transition from lead-based to lead-free solder materials driven by environmental regulations, understanding the mechanical properties and degradation mechanisms of these materials under thermal stress is essential.

2.1. Thermal Aging Mechanisms

Thermal aging of solder alloys, such as Sn-Ag-Cu (SAC) and other lead-free compositions, results in microstructural changes that significantly affect their mechanical properties. Studies by Mishra et al. (2015) highlight how prolonged exposure to elevated temperatures leads to intermetallic compound (IMC) formation at the solder/substrate interface, which can embrittle the joints and accelerate crack propagation. Li et al. (2016) further elaborate that aging can promote phase separation and growth of IMCs, altering the mechanical integrity of solder joints.

2.2. Crack Initiation and Growth

The initiation of cracks in solder joints is often linked to the accumulation of strain due to thermal cycling and stress. Shu et al. (2017) explored the effect of thermal cycling on the fatigue life of SAC solder and found that thermal aging exacerbates crack initiation due to microstructural coarsening. Similarly, Kim et al. (2018) demonstrated that the presence of IMCs, particularly Ag3Sn, can act as stress concentrators, facilitating crack propagation under cyclic loading conditions.

2.3. Mechanical Properties

The mechanical properties of lead-free solders, such as tensile strength and ductility, are adversely affected by thermal aging. Buchanan et al. (2019) reported a decrease in elongation and an increase in yield strength with aging, attributing these changes to grain growth and the development of brittle phases within the solder matrix. Zhang et al. (2020) examined the creep behavior of aged lead-free solder and found that thermal exposure led to a reduction in creep resistance, indicating a significant impact on long-term reliability.

2.4. Models of Crack Growth

Several models have been proposed to understand the crack growth behavior in solder interconnects. Paris and Erdogan’s (1963) crack growth model has been adapted for solder materials by researchers such as Khan et al. (2021), who incorporated thermal aging effects into their analysis. Their findings suggest that the modified Paris law can effectively predict crack propagation rates in aged solder joints, emphasizing the role of environmental factors in influencing crack dynamics.

2.5. Mitigation Strategies

To mitigate the effects of thermal aging on crack growth, various strategies have been investigated. Wang et al. (2022) explored the use of alloying elements and surface treatments to enhance the durability of lead-free solders. Their results indicated that the addition of small amounts of Bi can improve thermal stability and reduce crack propagation rates. Furthermore, Lee and Park (2023) highlighted the potential of nanostructured solder materials in improving the resistance to thermal aging, thus prolonging the lifespan of electronic devices.

III. METHODOLOGY

3.1 Material Characterization

For accurate simulations and forecasts, it is essential to comprehend the properties and composition of a material. The material characterization procedure is used to achieve this. This work focuses on characterizing key properties of materials used in electronic packages to improve the accuracy of finite element analysis (FEA) in ANSYS Workbench. Among the properties being looked at are Young's modulus (E), Poisson's ratio (v), and the coefficient of thermal expansion (CTE). Below is a more detaileddescription of the instruments and techniques utilized to obtain these measurements.

3.1.1 Thermo-Mechanical Analyzer (TMA)

Both the materials' CTE and Glass Transition Temperature (Tg) were determined using the

Thermo- Mechanical Analyzer (TMA)

- Thermal expansion coefficient (CTE): The coefficient of thermal expansion (CTE) measures a material's capacity to expand or compress. The definition of it is the fractional change in volume or length for every unit change in temperature. The following formula is applied:
- α=ϵΔT\alpha = \frac{\epsilon}{\Delta T}α=ΔTϵWhere:
    - α\alphaα – Coefficient of Thermal Expansion (ppm/°C)
    - ϵ\epsilonϵ – Strain (mm/mm)
    - ΔT\Delta TΔT – Temperature Difference (°C)

TMA measurements were performed using a Hitachi TMA 7000. PCB samples, measuring 8 mm x 8 mm,were subjected to a temperature range from -65°C to 260°C with a ramp rate of 5°C/min**Error! Reference source not found.**. The TMA setup is shown in **Figure 4**. CTE results for solder and PCB are plotted in **Figures 5** and **6**.

Table 1. CTE of Components

Material	CTE (ppm/^{o}C)
Copper Pad	17.78
Die Attach	65
Die	2.94
Mold	8.43
Polyimide Layer	35
Solder Mask	30

Table 2. CTE average from the plots

Material	CTE No aging	CTE aging 80	CTE aging 125
Board	1.34773E-05	1.26542E-05	1.25378E-05
Solder	0.001525735	0.001579035	0.001773808

Figure 4. TMA 7000

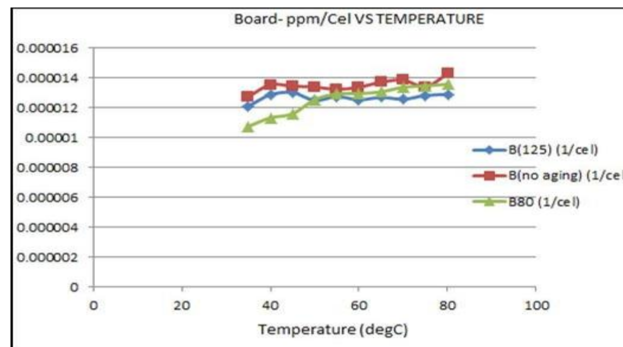

Figure 5. CTE Results for PCB

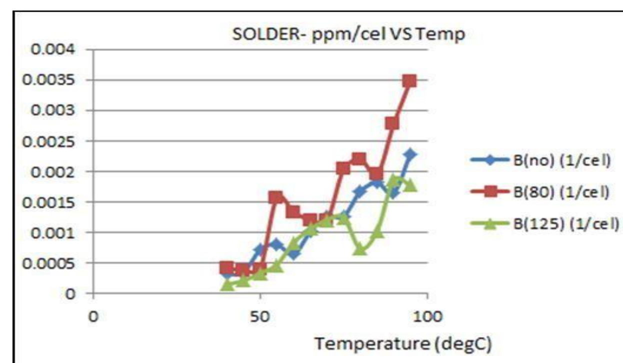

Figure 6. CTE Results for Solder

The temperature range a polymer changes from a hard, glassy state to a soft, rubbery state is known as the Glass Transition Temperature (Tg). To quantify this shift, the TMA tracks variations in the CTE plot's slope.

3.1.2 The DMA, or Dynamic Mechanical Analyzer

- The materials' complex modulus, loss modulus, and storage modulus were measured using the Dynamic Mechanical Analyzer (DMA)**Error! Reference source not found.**.
- Storage Modulus (E'): Indicates the stiffness of a material by representing the elastic part of its response. The storage modulus is the source of Young's modulus.E=σϵE = \frac{\sigma}{\epsilon}E=ϵσWhere:
  - EEE – Young's Modulus (MPa)
  - σ\sigmaσ – Stress (MPa)
  - ϵ\epsilonϵ – Strain (mm/mm)
- **Loss Modulus (E'')**: Represents the viscous portion of the material, indicating energydissipation as heat.
- **Complex Modulus (Ec)**: A combination of the storage and loss moduli. Ec=E'+i(E'')E_c = E' + i(E'')Ec=E'+i(E'') The Young's Modulus is calculated using: |Ec|=E=(E')2+(E'')2|E_c| = E = \sqrt{(E')^2 + (E'')^2}|Ec|=E=(E')2+(E'')2

A Hitachi DMA 7100 was used for the DMA tests. Samples with dimensions of 50 mm by 10 mm were clamped into a bending device. Figure 7 displays the DMA configuration. Figures 8 and 9 plot the solder and PCB Young's modulus results.

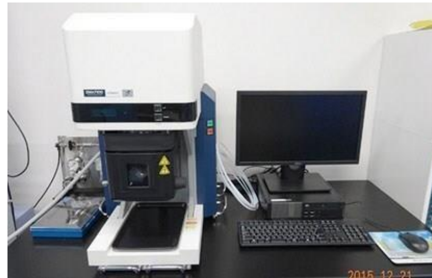

Figure 7. DMA Hitachi 7100

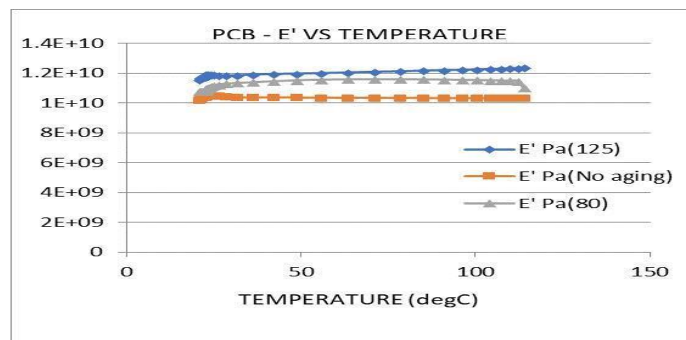

Figure 8. Young's Modulus of PCB

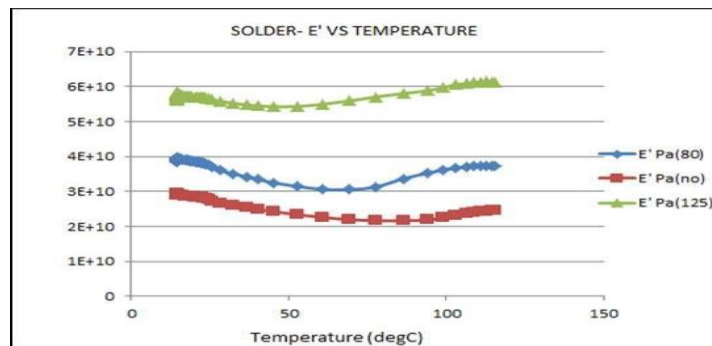

Figure 9. Young's Modulus of Solder

Table 3. Young's Modulus of Components

Material	Young's Modulus (Gpa)
Copper Pad	110
Die Attach	154
Die	150
Mold	24
Polyimide Layer	3.3
Solder Mask	4.6

Rover Publications
United International Journal of Engineering and Sciences (UIJES)
An International Peer-Reviewed (Refereed) Engineering and Science Journal
Impact Factor: 7.984 (SJIF) Vol-4, Issue- 2, 2024 ISSN: 2582-5887, www.uijes.com

Table 4. Young's Modulus Average from the Plots

Material	YM No Aging	YM aging 80	YM aging 125
Board	10423179854	10998546143	11890821241
Solder	37882151491	37882151491	57586777525

3.2 Temperature Chamber

Isothermal aging conditions were simulated using a temperature chamber. The chamber exposes materials to high temperatures and has a visible 12" x 4" borosilicate glass top wall. In Figure 10, the chamber configuration is displayed. The samples were subjected to 80°C and 125°C temperatures for three and five days, respectively.

Figure 10. Temperature Chamber

3.3 X-Ray Spectroscopy

X-ray spectroscopy was utilized to examine the materials' elemental makeup. With this method, atoms are excited with high-energy beams (protons, electrons, or X-rays), and the elemental composition of the atoms is ascertained by examining the X-rays that are released. Figure 11 presents the X-ray spectroscopy data. Wavelength dispersive X-ray spectroscopy (WDS) and energy-dispersive X-ray spectroscopy (EDS) are two of the methods employed.

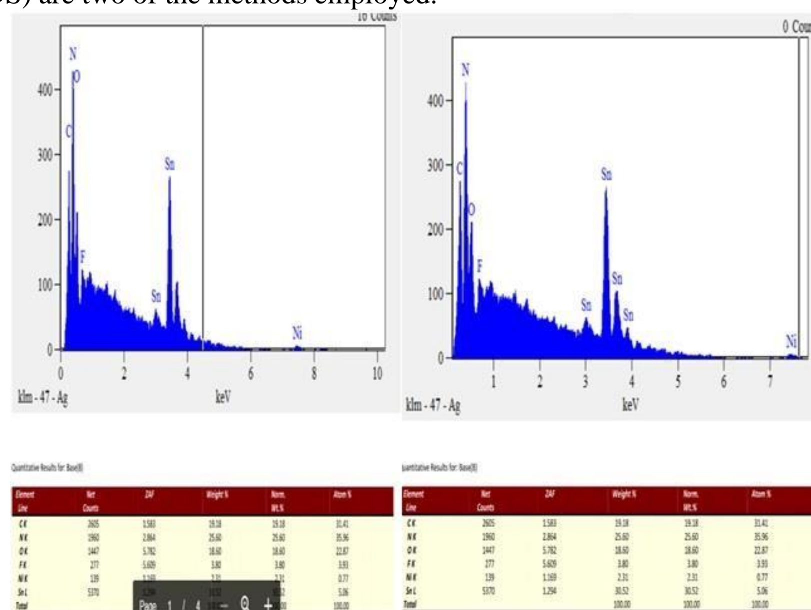

Element Line	Net Counts	ZAF	Weight %	Norm. Wt.%	Atom %
C K	2605	1.583	19.18	19.18	31.41
N K	1960	2.864	25.60	25.60	35.96
O K	1447	5.782	18.60	18.60	22.87
F K	277	5.609	3.80	3.80	3.93
Ni K	139	[illegible]	[illegible]	2.31	0.77
Sn L	5370	[illegible]	[illegible]	[illegible]	5.06
Total			[illegible]	[illegible]	100.00

Element Line	Net Counts	ZAF	Weight %	Norm. Wt.%	Atom %
C K	2605	1.583	19.18	19.18	31.41
N K	1960	2.864	25.60	25.60	35.96
O K	1447	5.782	18.60	18.60	22.87
F K	277	5.609	3.80	3.80	3.93
Ni K	139	1.169	2.31	2.31	0.77
Sn L	5370	1.294	30.52	30.52	5.06
Total			100.00	100.00	100.00

Figure 11. Results of X-Ray Spectroscopy

Impact Factor: 7.984 (SJIF) Vol-4, Issue- 2, 2024 ISSN: 2582-5887, www.uijes.com

III. MODELLING FINITE ELEMENTS

Finite Element Modelling (FEM) is a sophisticated numerical method used extensively in engineering to solve complex problems involving structural, thermal, and fluid dynamics. This section provides an overview of FEM, its applications, and the detailed steps involved in performing FEM analysis.

4.1 Engineering Applications of FEM

FEM is a flexible tool that is applied to a wide range of issues in different engineering domains. Aerospace, mechanical, civil, automotive, structural analysis (static, dynamic, linear, non-linear), thermal and fluid flow analysis, nuclear engineering, electromagnetic analysis, biomechanics and geomechanics, biomedical engineering, hydraulics, and other fields are among the major uses.

4.2 Structural Analysis

Structural analysis aims to compute deformations, internal forces, and stresses in a structure. Key types of structural analysis include:

- Static Analysis: Calculates stresses and displacements under conditions of static loading.
- Modal analysis: Determines a structure's natural frequencies and mode shapes.
- Harmonic Analysis: Evaluates how a structure reacts to loads that change over time.
- Transient Dynamic Analysis: Examines how a system reacts to random loads that fluctuate over time.
- Spectrum Analysis: Determines strains and stresses using random vibrations or response spectra.
- Buckling Analysis: Assesses patterns of deformation and buckling loads.
- Advanced Structural Analysis: Investigates non-linear behavior, stability, and dynamic reactions.

4.3 Thermal Analysis

Thermal analysis helps in calculating temperature gradients, heat transfer, and thermal fluxes. It includes:

- Steady-State Thermal Analysis: Determines thermal quantities under static loading conditions.
- Transient Thermal Analysis: Assesses thermal behavior under time-varying conditions.

4.4 Steps in FEM

The process of FEM analysis involves several key steps, each contributing to the overall solution of theproblem.

4.4.1 Discretization

The first step in FEM is discretization, where the problem domain is divided into smaller, manageable elements connected at nodes. This process includes:

- Element and Node Numbering: Proper numbering affects computational efficiency, as it influences the bandwidth of the global stiffness matrix.
- Optimization: FEM programs often perform internal numbering to minimize bandwidth and optimize computation.

4.4.2 Element Analysis

Element analysis involves:

- Displacement and Equilibrium: Displacements within elements are expressed using shape functions, and equilibrium is maintained.
- Stress-Strain Relationship: The stress-strain relationship is derived using the element stiffness matrix S=K·VS = K \cdot VS=K·V.

4.4.3 System Analysis

System analysis combines contributions from individual elements to establish:

- Global Stiffness Matrix: Assembled from element stiffness matrices.
- Load Vector: Obtained from known nodal forces.

4.4.4 Boundary Conditions

Boundary conditions are applied by setting known nodal displacements or adding spring stiffness values.

4.4.5 Finding Global Displacements

Global displacements are calculated by solving the linear system:

r=K−1(R−R0)r = K^{-1} (R - R_0)r=K−1(R−R0)

4.4.6 Calculation of Stresses

Stresses are derived from strains using Hooke's law:

σ(x,y,z)=D·B(x,y,z)·V\sigma(x, y, z) = D \cdot B(x, y, z) \cdot Vσ(x,y,z)=D·B(x,y,z)·VWhere:

- DDD – Hooke's law matrix
- BBB – Strain-displacement matrix
- VVV – Displacement vector

4.5 Submodelling

Submodelling is used to refine mesh resolution in regions of interest within a larger model. This technique involves:

- Creating Finer Meshes: Focuses on specific areas for more accurate results.
- Cut Boundary Displacement Method: Uses displacements from a coarse model as boundary conditions for a submodel.

Figure 12 illustrates the submodelling method with (a) a coarsely meshed model and (b) a finely meshed sub-model.

Advantages of Submodelling:

- Reduces Need for Complex Transitions: Simplifies modeling in regions of interest.
- Facilitates Design Optimization: Allows experimentation with different design parameters.
- Improves Mesh Refinement Verification: Helps validate mesh quality.

Limitations of Submodelling:

- Valid for Solid and Shell Elements Only: Restricted to specific element types.
- Boundary Distance Requirement: Assumes boundaries are sufficiently distant from stress concentrations.

Figure 13 provides a fundamental overview of submodelling principles.

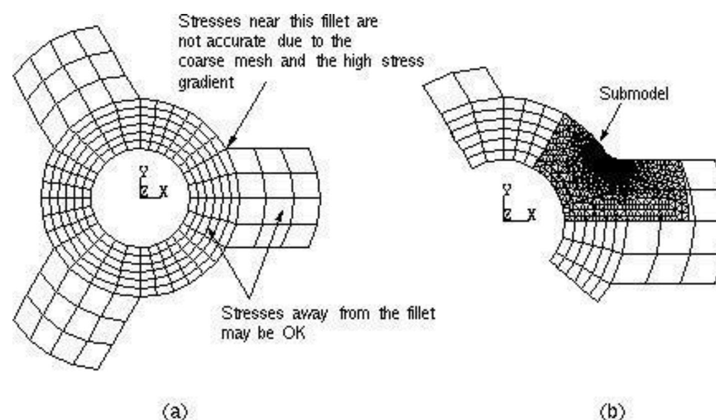

Figure 12. Sub-modelling Method

Rover Publications
United International Journal of Engineering and Sciences (UIJES)
An International Peer-Reviewed (Refereed) Engineering and Science Journal
Impact Factor: 7.984 (SJIF) Vol-4, Issue- 2, 2024 ISSN: 2582-5887, www.uijes.com

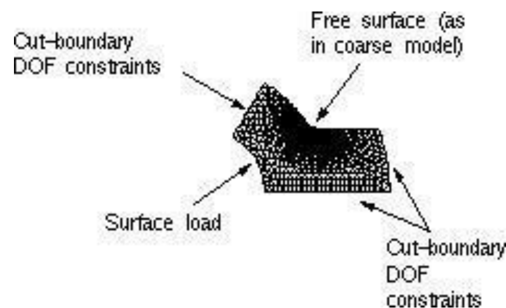

Figure 13. Sub-modelling Fundamentals

IV. MODELLING, METHODOLOGY AND SIMULATION

This section describes the finite element (FE) modeling, simulation, and technique used to examine how thermal aging affects the behavior of fracture formation in lead-free solder interconnects and how that behavior affects package dependability. The procedure is divided into discrete sections for the phases of processing, solution, and post-processing.

5.1 Processing

The processing phase is divided into three main steps:

5.1.1 Modeling the Geometry

The silicon die, which is inserted into a mold and connected to a substrate solder mask with a die attach, provides the geometry for the package. The substrate solder mask is attached to a polyimide layer, and copper pads are placed on the top and bottom surfaces of the solder balls. The dimensions of the various package components are listed in Table 5, and a detailed illustration of the Ball Grid Array (BGA) packaging is presented in Figure 14. The model has an 11x11 array of Micro Star BGA and simulates with ANSYS 18.

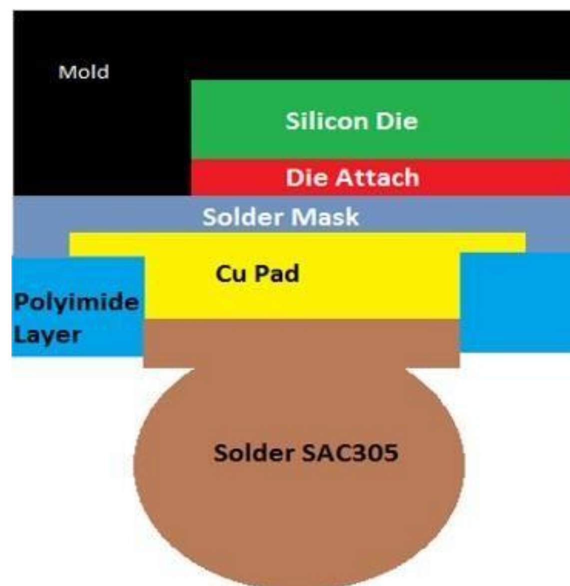

Figure 14. Detailed Drawing of a BGA Package

Table 5. Package Detailed Dimensions

Component	Dimensions (mm)
Package	6 x 6 x 0.74
Die	4.5 x 4.5 x 0.28
Solder Ball Pitch	0.5
Solder Ball Diameter	0.3
Solder Ball Height	0.2
Solder Mask Thickness	0.05
Substrate Thickness	0.05
Copper Pad Thickness	0.04

A sub-model derived from the global model is utilized for focused analysis, as depicted in **Figures 16** and **17**.

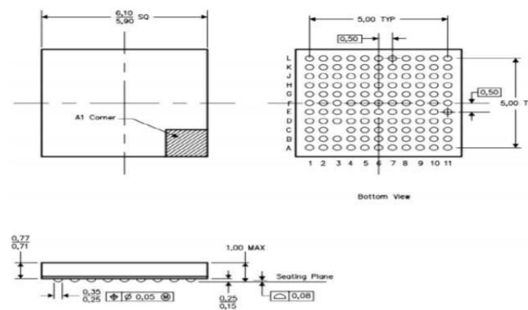

Figure 15. Schematic Diagram of BGA

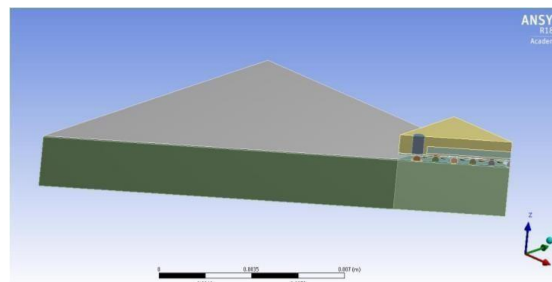

Figure 16. Octant Symmetry Model

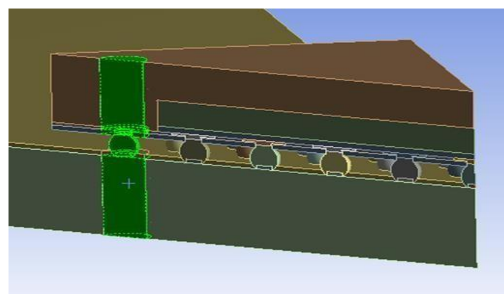

Figure 17. Exploded Sub-Model Highlighting Crack Locations

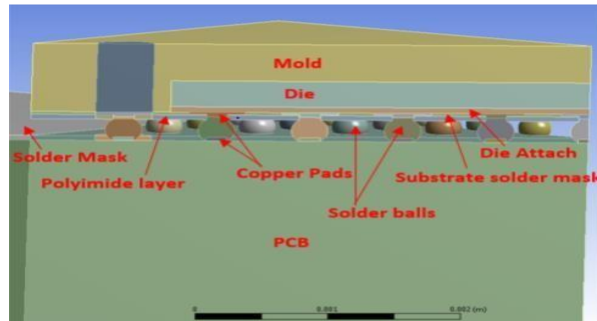

Figure 18. Cross-section of Geometry

5.1.2 Assigning Material Properties

Based on presumptions, the material attributes for the model are assigned. With the exception of solder balls, the package materials are handled as linearly elastic, and Anand's Viscoplastic Model is used to model the solder as a rate-dependent viscoplastic material. Shear modulus, Young's modulus, Poisson's ratio, and temperature-dependent coefficients of thermal expansion (CTE) are among the characteristics of the material. SAC305 solder is made up of 0.5% Copper (Cu), 3% Silver (Ag), and 96.5% Tin (Sn). The overall strain is stated as follows:

$$\epsilon_{ij} = \epsilon_{eij} + \epsilon_{in}$$

Anand's viscoplastic model defines the inelastic strain rate as:

$$\frac{d\epsilon_{in}}{dt} = \xi \cdot \sigma \cdot e^{\left(\frac{-Q}{RT}\right)}$$

where $d\epsilon_{in}/dt$ is the effective inelastic strain rate, σ is the effective true stress, and ***T*** is the absolute temperature.

$$\frac{d\varepsilon_{in}}{dt} = A\left[\sin h\left(\xi\,\frac{\sigma}{s}\right)\right]^{\frac{1}{m}} \exp\left(-\frac{Q}{RT}\right)$$

$$\dot{s} = \left\{h_0(|B|)^{\alpha}\,\frac{B}{|B|}\right\}\frac{d\varepsilon_p}{dt}$$

$$B = 1 - \frac{s}{s^*}$$

$$s^* = \hat{s}\left[\frac{1}{A}\,\frac{d\varepsilon_p}{dt}\exp\left(-\frac{Q}{RT}\right)\right]$$

Table 6: Anand's Constants for SAC 305

Constant	Name	Unit	Value
S_0	Initial Deformation Resistance	MPa	12.41
Q/R	Activation Energy/ Universal Gas Constant	1/K	9400
A	Pre-exponential Factor	Sec−1^{-1}−1	4E+06
ξ	Multiplier of Stress	Dimensionless	1.5
m	Strain Rate Sensitivity of Stress	Dimensionless	0.303

h_0	Hardening/Softening Constant	MPa	1378.8
s_o	Coefficient of Deformation Resistance Saturation	MPa	0.07
n	Strain Rate Sensitivity of Saturation	Dimensionless	1.3
a	Strain Rate Sensitivity of Hardening or Softening	Dimensionless	1.6832

5.1.3 Mesh Generation

Because of the semi-elliptical fracture portrayal, the solder ball has tetrahedral meshing, while the remainder of the model has hex-dominant meshing. The important solder ball is the one that is placed furthest from the neutral point, or the center of the package. The meshing of the exploding sub-model, which has 934,544 nodes overall and 4,488,799 elements, is depicted in Figure 19.

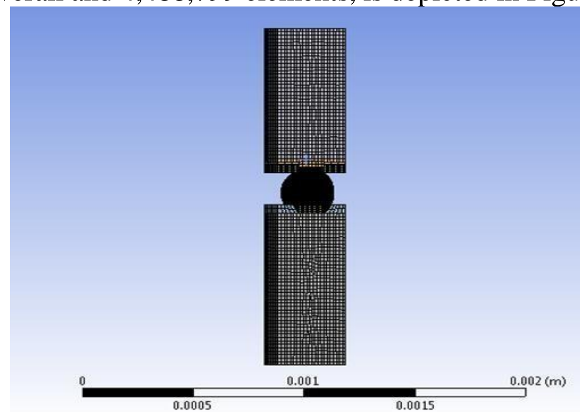

Figure 19. Meshing of Exploded Sub-model

5.2 Solution

The solution phase consists of four key sub-steps:

5.2.1 Application of Loads and Boundary Conditions

The package is subjected to loads that cycle with heat. The symmetric boundary requirements for the octant symmetry faces provide frictionless support for the symmetric faces and lock the common vertex at zero degrees of freedom (DOF). For the sub-model, only frictionless support is employed.

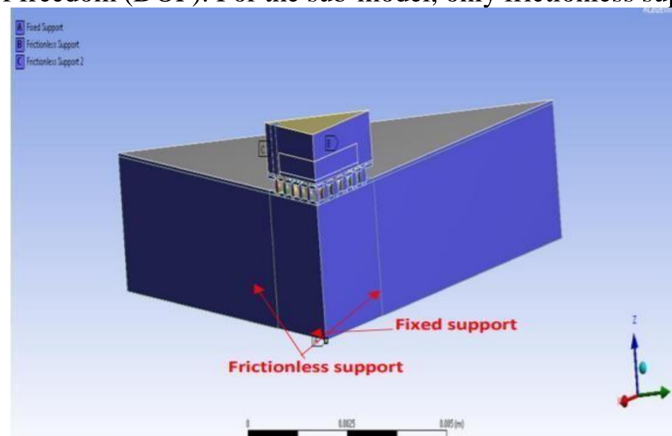

Figure 20. Boundary Conditions in ANSYS 18.0

Figure 21. Sub-modelling Boundary Condition

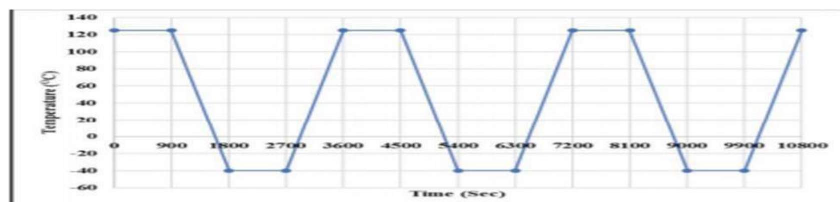

Figure 22. Thermal Cycling Profile

5.2.2 Selection of Output and Load Step Controls

Specific output variables, such as elastic strain, normal and shear stresses, and principal stresses, are defined for evaluation at various load steps.

5.2.3 Selection of Solver

ANSYS 18's solvers are employed to obtain solutions for the modeled system, ensuring convergence and accuracy in the results.

5.2.4 Obtaining the Solution

The solution results are processed to extract relevant data for analysis.

5.3 Post Processing

Post-processing involves reviewing and analyzing the results obtained from the simulations. Critical points of maximum elastic strain, normal and shear elastic strain, normal stress, maximum principal stress, and principal elastic strain are evaluated.

Figure 23 shows the details of the semi-elliptical crack representation, with specific crack locations on the solder interconnects identified for analysis. These cracks were strategically modeled based on maximum stress and strain points identified during thermal cycling conditions. Other cracks, not at critical locations, were modeled randomly to assess their impact on reliability.

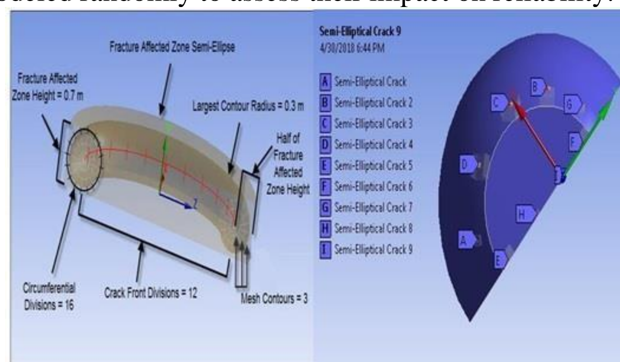

Figure 23. Semi-elliptical Crack Fundamentals

Through this modeling and simulation framework, we aim to establish a comprehensive understanding of the crack growth behavior in lead-free solder interconnects under thermal aging conditions, thereby contributing to enhanced reliability assessments of electronic packages.

V. RESULTS AND DISCUSSION

This chapter presents the findings from the fracture analysis of solder interconnects subjected to thermal cycling, post thermal aging, using ANSYS Workbench v18.0. The primary goal was to identify critical cracks, their locations, and modes of failure to highlight areas where cracks may develop, thereby saving experimental costs and time. Key results include J-integral values, Stress Intensity Factors (SIF), plastic work, and cycles to failure, providing insight into the reliability of solder interconnects under thermal stress.

6.1 Results

6.1.1 J-Integral (J/m²) Results

The J-integral values were computed for various cracks in the models under different aging conditions.The results are summarized in the tables below:

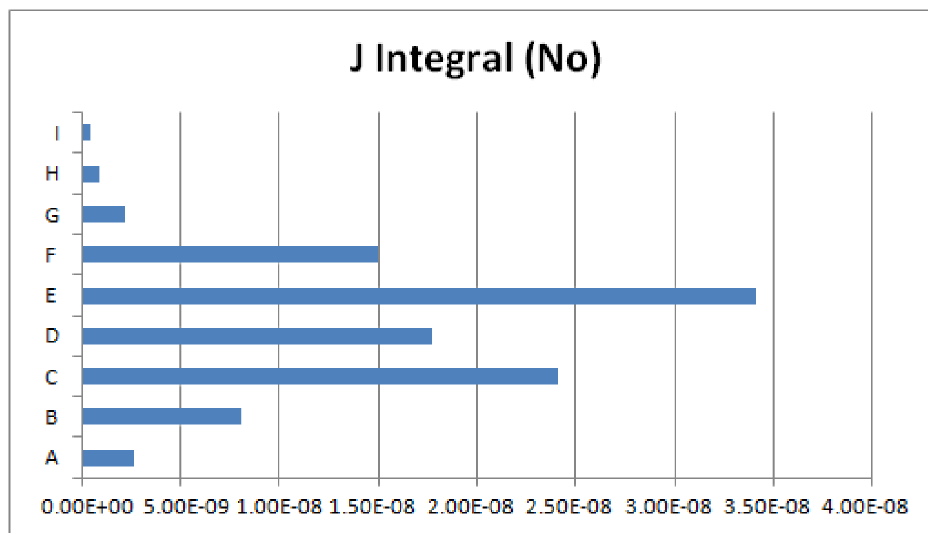

Figure 24. J-Integral for No Aging Model

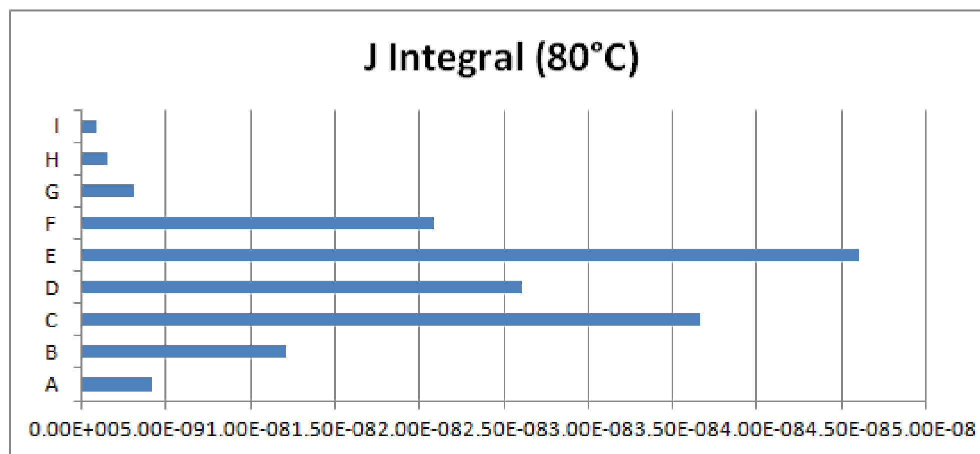

Figure 25. J-Integral for 80°C Aged Model

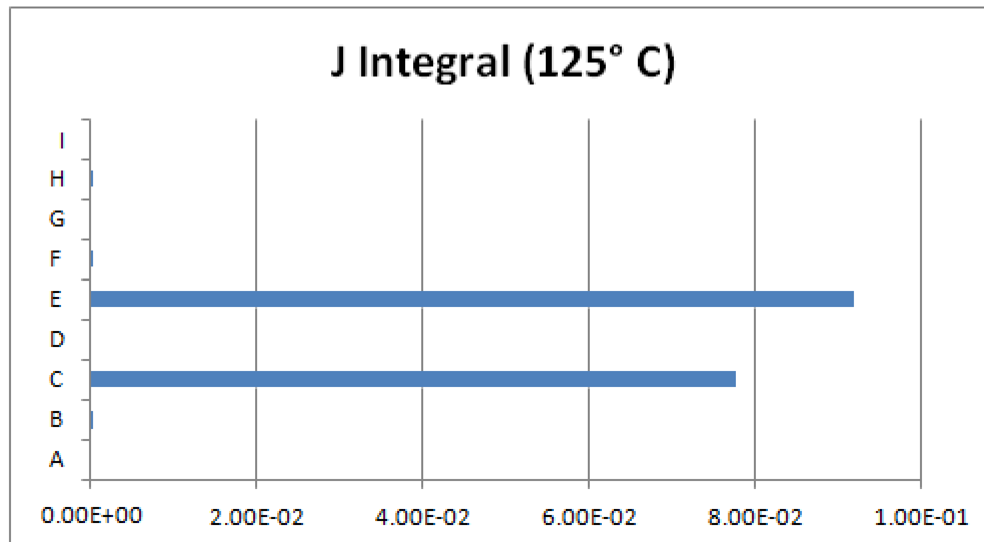

Figure 26. J-Integral for 125°C Aged Model

6.1.2 Stress Intensity Factor (SIF) Results

The calculated Stress Intensity Factors (SIF) under varying aging conditions are presented below.

Table 7. SIF for No Aging Model (Pa*m^0.5)

Crack	A	B	C	D	E	F	G	H	I
K1 (No Aging)	609.53	2720	1898.6	763.4	8715.4	20425	1627.9	-2068	-1870.1
K2 (No Aging)	415.9	33.1	933.9	464.05	13689	20196	965.5	220.81	147.26
K3 (No Aging)	2369.3	2565.2	2698.2	2539.1	15044	26677	3316.1	220.81	-21.258

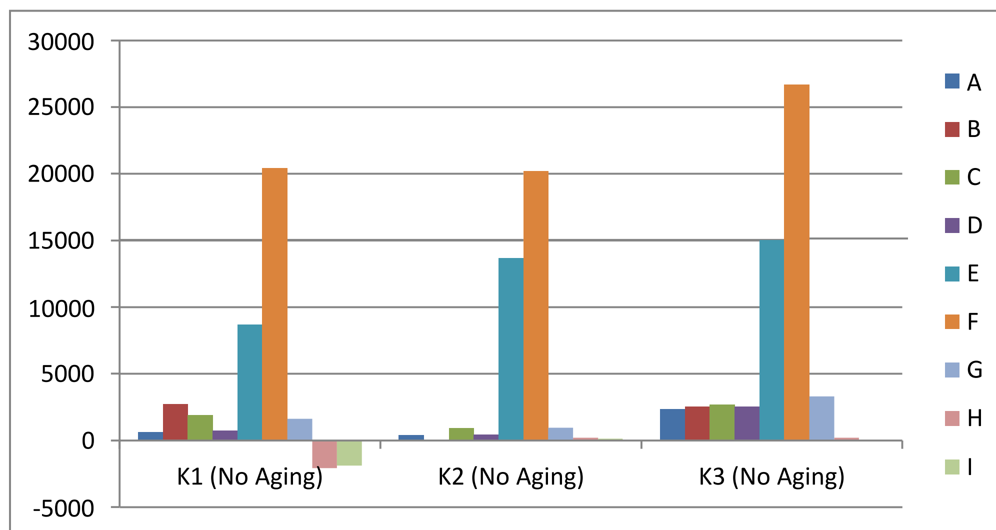

Figure 27. SIF for No Aging Model

Rover Publications
United International Journal of Engineering and Sciences (UIJES)
An International Peer-Reviewed (Refereed) Engineering and Science Journal
Impact Factor: 7.984 (SJIF) Vol-4, Issue- 2, 2024 ISSN: 2582-5887, www.uijes.com

Table 8. SIF for 80°C Aged Model (Pa*m^0.5)

Crack	A	B	C	D	E	F	G	H	I
K1 (80°C)	-11.168	6.1655	39.082	14.654	15.043	18.231	-11.679	-3.4431	-3.0322
K2 (80°C)	6.5184	29.922	15.882	31.174	54.548	55.153	12.939	150.73	148.23
K3 (80°C)	-0.6489	18.513	6.969	-10.502	461.68	461.87	-3.3607	65962	65971

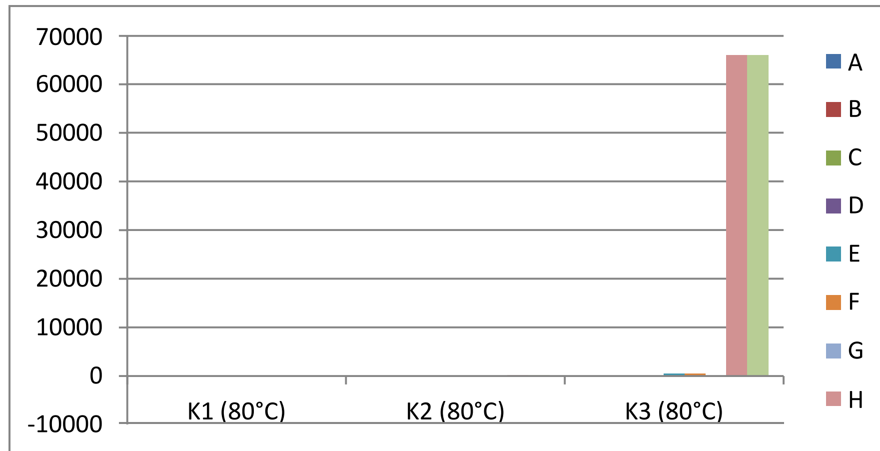

Figure 6-5: SIF for 80°C Aged Model

Table 9. SIF for 125°C Aged Model (Pa*m^0.5)

Crack	A	B	C	D	E	F	G	H	I
K1 (80°C)	-11.168	6.1655	39.082	14.654	15.043	18.231	-11.679	-3.4431	-3.0322
K2 (80°C)	6.5184	29.922	15.882	31.174	54.548	55.153	12.939	150.73	148.23
K3 (80°C)	-0.6489	18.513	6.969	-10.502	461.68	461.87	-3.3607	65962	65971

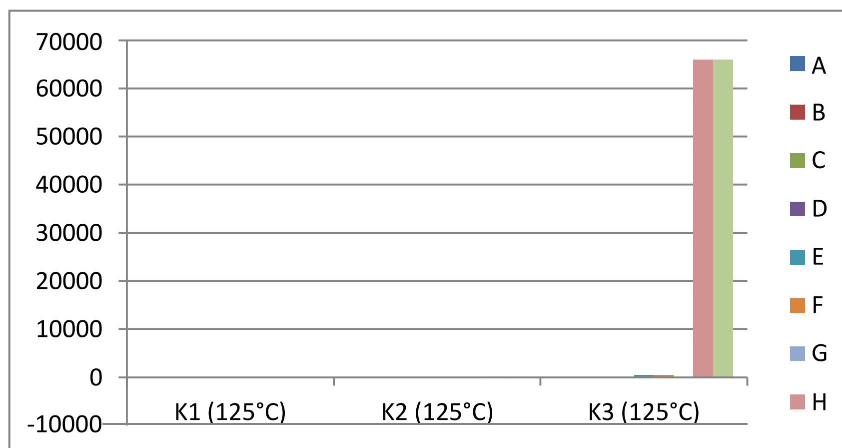

Figure 6-6: SIF for 125°C Aged Model

Negative values of SIF indicate that cracks may propagate under compressive loads. Notably, if the SIFKKK is less than the fracture toughness KcK_cKc, crack propagation will not occur.

6.1.3 Cycles to Failure

Volume-averaged plastic work was correlated with cycles to failure using Syed's Model:

$Nf = (/ \Delta W)^k$

6.2 Conclusion

ANSYS Workbench 18.0 was used to successfully create a 3D model of a BGA package. The reliability of thermal cycling is considerably reduced by thermal aging, as evidenced by the identification of critical cracks and associated causes of failure. A shorter package lifespan was connected with an increase in aging temperature. Based on the study, fracture E was identified as the critical fracture because it had the highest J-integral and a failure propensity at the sites of maximal elastic strain. Furthermore, it was shown that break C was the second most significant break, highlighting the significance of maximal elastic strain in solder interconnect fracture investigations.

This study has provided a comprehensive analysis of the impact of thermal aging and thermal cycling on the crack growth behavior of lead-free solder interconnects, specifically focusing on SAC solders widely used in electronic packaging. The findings demonstrate that thermal aging significantly alters the microstructure and mechanical properties of solder joints, which in turn affects their reliability and performance. Through a combination of experimental testing and finite element analysis, we established a clear relationship between stress intensity factors, crack dimensions, and thermal loading conditions. The results underscore the critical importance of understanding crack propagation mechanisms to enhance the longevity and reliability of electronic packages.

The integration of advanced modeling techniques, such as the multi-level finite element approach, has not only reduced experimental time and costs but also improved the predictive capabilities regarding solder joint behavior under varying thermal conditions. This research contributes valuable insights into the mechanical responses of solder interconnects, paving the way for more reliable designs in electronic packaging.

6.3 Future Work

Building upon the findings of this study, several avenues for future research can be identified:

- Long-term Reliability Studies: Further investigations are needed to assess the long-term effects of thermal aging on solder joints under real-world operating conditions. These studies should include accelerated aging tests that mimic environmental stressors, such as humidity and mechanical vibrations.
- Microstructural Analysis: Advanced characterization techniques, such as scanning electron microscopy (SEM) and transmission electron microscopy (TEM), can be employed to provide a more detailed understanding of microstructural changes in solder joints over time, particularly regarding the formation and growth of intermetallic compounds.
- Diverse Solder Alloys: Future research could explore the performance of alternative lead-free solder alloys, evaluating their fatigue behavior and reliability compared to SAC solders. This wouldhelp identify materials that offer improved performance in specific applications.
- Modeling Improvements: Continued development of the finite element models, including the incorporation of more complex loading scenarios and geometries, will enhance the accuracy of predictions regarding crack propagation and failure modes.
- Experimental Validation: Further experimental validation of the finite element models with a focus on real-time monitoring of crack growth in solder interconnects during thermal cycling and mechanical loading could provide deeper insights into the failure mechanisms.
- Impact of Manufacturing Processes: Investigating how different manufacturing processes (e.g., reflow profiles, PCB surface treatments) influence solders joint reliability would be beneficial.

Understanding these relationships could lead to optimized manufacturing practices that enhance the durability of electronic packages.

V. REFERENCES

[1] Karnik, Anuraag Girish, "IMPACT OF THERMAL AGING ON CRACK GROWTH BEHAVIOR OF LEAD FREE SOLDER INTERCONNECTS" (2018). Mechanical and Aerospace Engineering Theses. 843. https://mavmatrix.uta.edu/mechaerospace_theses/843

[2] Zhang, J., et al. (2013). Thermal aging effects on the thermal cycling reliability of lead-free fine pitch packages. IEEE Transactions on Components, Packaging and Manufacturing Technology, 3(8), 1348-1357. https://doi.org/10.1109/TCPMT.2013.2272335

[3] Motalab, M., et al. (2013). Correlation of reliability models including aging effects with thermal cycling reliability data. In 2013 IEEE 63rd Electronic Components and Technology Conference (pp. 986-1004). Las Vegas, NV. https://doi.org/10.1109/ECTC.2013.6557812

[4] Xu, L., Pang, J. H. L., Prakash, K. H., & Low, T. H. (2005). Isothermal and thermal cycling aging on IMC growth rate in lead-free and lead-based solder interface. IEEE Transactions on Components and Packaging Technologies, 28(3), 408-414. https://doi.org/10.1109/TCAPT.2005.853156

[5] Yang, D., & Cui, Z. (2011). The effect of thermal aging on the mechanical properties of molding compounds and the reliability of electronic packages. In Proceedings of the 2011 International Conference on Electronic Packaging Technology (pp. 1-4). https://doi.org/10.1109/ICEPT.2011.6067004

[6] Rodgers, B., Punch, J., & Jarvis, J. (2002). Finite element modelling of a BGA package subjected to thermal and power cycling. In ITherm 2002. Eighth Intersociety Conference on Thermal and Thermomechanical Phenomena in Electronic Systems (pp. 993-1000). https://doi.org/10.1109/ITHERM.2002.1023641

[7] Lau, J. H. (1996). Solder joint reliability of flip chip and plastic ball grid array assemblies under thermal, mechanical, and vibrational conditions. IEEE Transactions on Components, Packaging, and Manufacturing Technology: Part B, 19(4), 728-735. https://doi.org/10.1109/6144.541903

[8] Raju, S., & Newman, J. C. (1980). Stress-intensity factors for a wide range of semi-elliptical surface cracks in finite-thickness plates. NASA-Langley Research Center.

[9] Begley, J., & Landes, J. (1972). The J integral as a fracture criterion. In H. Corten (Ed.), Fracture Toughness: Part II (pp. 1-23). ASTM International. https://doi.org/10.1520/STP38816S-1

[10] Rahangdale, U., et al. (2017). Damage progression study of 3D TSV package during reflow, thermal shocks, and thermal cycling. In 2017 16th IEEE Intersociety Conference on Thermal and Thermomechanical Phenomena in Electronic Systems (ITherm) (pp. 1119-1125). Orlando, FL. https://doi.org/10.1109/ITHERM.2017.7992003

[11] Yu, Q., Kikuchi, H., Ikeda, S., Shiratori, M., Kakino, M., & Fujiwara, N. (2002). Dynamic behavior of electronics package and impact reliability of BGA solder joints. In ITherm 2002. Eighth Intersociety Conference on Thermal and Thermomechanical Phenomena in Electronic Systems (pp. 953-960). https://doi.org/10.1109/ITHERM.2002.1023640

[12] Wang, T. H., & Lai, Y. S. (2005). Submodeling analysis for path-dependent thermomechanical problems. Journal of Electronics Packaging, 127(4). https://doi.org/10.1115/1.2138126